Journal of Advanced Research in Fluid Mechanics and Thermal Sciences

Journal homepage:
https://semarakilmu.com.my/journals/index.php/fluid_mechanics_thermal_sciences/index
ISSN: 2289-7879

Cellulose Acetate/Polyethylene Glycol Composite Beads for Efficient Removal of Methylene Blue

Hikmatun Ni'mah[1,*], Fira Rizky Ramadhan[1], Talitha Adella Assegaf[1], Citra Kartika Asri[1], Nurul Rahmawati[1], Firman Kurniawansyah[1]

[1] Department of Chemical Engineering, Faculty of Industrial Technology and System Engineering, Institut Teknologi Sepuluh Nopember (ITS), Surabaya, East Java, 60111, Indonesia

ARTICLE INFO

Article history:
Received 25 May 2023
Received in revised form 21 July 2023
Accepted 30 July 2023
Available online 15 August 2023

Keywords:
Cellulose acetate; polyethylene glycol; adsorbent; methylene blue; composite bead

ABSTRACT

The development of eco-friendly and biodegradable adsorbent with excellent adsorption performance is of great importance for the efficient dye removal in wastewater. Herein, an efficient and biodegradable composite adsorbent bead was fabricated from cellulose acetate (CA) modified with low molecular weight polyethylene glycol 200 (PEG200) for the adsorptive removal of methylene blue dye (MB) from aqueous solution. The weight fraction of PEG was varied to investigate the effect of material bead composition on the morphology, molecular structure, crystal phases, thermal stability, mechanical properties, and adsorption performance of the composite beads. Batch adsorption was carried out at various times to estimate the time at equilibrium adsorption capacity and kinetic model. Various operating conditions such as pH, initial MB concentration, and adsorbent dosage in experiment were also executed to examine the adsorption performance of this system. The result showed that all beads have porous structure and the pore size increase after the addition of PEG200. The adsorption capacity and % MB removal generally showed an improvement with the rise of PEG content. The batch adsorption experiments demonstrated that the best % removal and adsorption capacity of MB were 93.35 % and 28.005 mg/g, respectively, that was obtained by composite CA/PEG200 (80/20) bead at pH of 11, initial MB concentration of 30 mg/L, and bead dosage of 1 g/L. The adsorption kinetic fitted well to Elovich-kinetic model with average R^2 of 0.844. Overall, this work offers new finding into the development of effective, environmentally friendly, and inexpensive cellulose-based adsorbents for wastewater remediation.

1. Introduction

The increasing of industrialization, along with the increase in human population, has a severe impact on environmental pollution, especially water pollution. Water pollution can be caused by toxic heavy metals, anions, inorganic, micropollutants, and organic compounds such as dyes, phenols, pesticides, humus elements, and detergents. These pollutants considerably impact the ecology and

---

[*] *Corresponding author.*
E-mail address: hikmatun_n@chem-eng.its.ac.id

https://doi.org/10.37934/arfmts.108.2.3147

harm the ecosystem, flora, and fauna. Many of these pollutants are not easily degraded. Therefore, it is necessary to carry out treatment of contaminated water before being released to a broader area of the earth [1].

The textile industries consume more than 10 million kilograms of dye annually worldwide [2,3], with nearly 1 million kilograms of dye thrown into the water. When this pollutant dyes have been released into water body, it is no longer good condition for water environment. Consequently, it is challenging to remove the pollutant dyes because they have a complex molecular, causing stable and difficult to be degraded. Moreover, ordinary people usually judge water quality based on its color. The color of water is the first thing when assessing water quality. Because some types of dye are easily noticeable when they are present in water, even at low concentration of 1 ppm, which is not desirable [4]. Some technologies used to reduce pollutants in water include oxidation and reduction, separation with membrane, liquid extraction, ion exchange, coagulation, evaporation, crystallization, and adsorption. Each of these methods differs in their effectiveness in reducing pollutants and costs. Among of these various separation methods, the adsorption method is an effective method used to remove pollutants in wastewater, because it gives good results with a high level of efficiency for pollutant removal. This approach also uses a simple design process and equipment [4].

The most common adsorption process in wastewater treatment used activated carbon as the adsorbent, because it has a high-efficiency level and does not produce harmful by-products. However, activated carbon has non-biodegradable properties, which means activated carbon cannot be recycled. Therefore, it is necessary to develop innovations for biodegradable and recycled adsorbents [4]. Instead of modifying the polymer chain, adding additives such as polyethylene glycol (PEG) has been reported to increase the beads' hydrophilic properties. Earlier research by Idris *et al.,* [5], regarding to the membrane dialysis using CA (Cellulose Acetate) as raw material, reported that the effect of PEG addition has proven to enhance the membrane performance. Membrane performance in binding with solute is strongly influenced by PEG addition and its molecular weight [5]. PEG is one of the most common carriers used as an additive in a drug-matrix complex mixture to increase drug dissolution. PEG is one type of polymer that can form complex polymers on organic molecules when it is added into complex mixture, forming complexes with any drugs, to increase the rate of dissolution. Moreover, PEG itself can act as inert material and is not accessible to hydrolyzing.

Cellulose and its derivatives can be prepared in the form of spherical bead and applied as adsorbent. Cellulose beads were prepared by dissolving cellulose derivatives (viscose, cellulose ester, or ether) in their solvent and then regenerated by dropping slowly in a coagulation bath. The chemical composition of this regenerated cellulose bead was adjusted to perform de-derivatization form, which has been used in various applications. Because, cellulose beads have several distinctive properties, such as product availability and affordable price, spherical shape, possibility to adjust the particles size, mechanical strength (low-pressure loss in column, possibility to be applied as industrial filters), high porosity (accessibility for high molecular mass compounds), hydrophilicity (tolerance of biological structures, fast kinetics) and chemical reactivity in derivatizations [6]. Moreover, cellulose beads have porous structure, which are suitable as adsorbent.

Our previous studies observed the preparation of composite cellulose-based beads from the mixture of cellulose acetate butyrate (CAB) and poly(L-lactic acid) (PLLA) and their application as adsorbent in both batch and continuous adsorption systems [7-9]. The addition of PLLA improved the adsorption efficiency since the morphology of composite bead become more porous. In addition, the concentration of polymer solution, which influence the morphology of the beads, were also considered to affect the adsorption capacity and % removal of the MB. Researches conducted by Rofaudin et al., and Caesario *et al*., [8,9] on the continuous adsorption of dyes by composite beads from CAB and PLLA showed that pure CAB and CAB/PLLA composite beads affect the morphology, adsorption capacity and % removal from beads. Pure CAB bead have more porous morphology with larger surface area than CAB/PLLA composite beads. However, the pore size in cellulose beads become bigger after the addition of PLLA, contributing to better adsorption performance. The utilization of PLLA in the blend was motivated by its moderate properties such as biodegradability and excellent mechanical properties [10,11]. Thus, the composite beads are also biodegradable and better in mechanical properties.

In this research, cellulose beads were prepared from pure cellulose acetate (CA) and the mixture of CA and polyethylene glycol 200 (PEG200) and applied as adsorbents for adsorption of cationic dye methylene blue (MB) in batch system. CA is one of cellulose derivatives that can also be prepared as cellulose beads with porous structured morphology [12]. The addition of PEG200 is expected to modify the morphology of cellulose beads. PEG200 was reported by Ni'mah *et al.,* [11] to have an effect of promoting the formation of pores in PLLA structure. Therefore, in this current study, the effect of PEG200 addition in CA matrix in the formation of cellulose beads was evaluated on the adsorption of MB. To the best of our knowledge, this system of adsorbent was never studied yet. The effect of operational conditions on the adsorption performance of composite cellulose beads for MB removal was also analyzed. An evaluation of kinetic models suitable to describe the batch adsorption of MB was also carried out. In addition, the cationic dye methylene blue (MB) was used as adsorbate in this current research. MB is a dark green crystalline form, odorless, stable when in contact with air, and will produce a thick blue color. The MB is also soluble in water or alcohol and has a melting point of 100-110°C, a density of 1 gr/ml at a temperature of 20°C, and a solubility of 43.6 gr/L in water at 25°C [13]. MB is a cationic dye compound with the formula $C_{16}H_{18}ClN_3XH_2O$. This compound is called basic blue 9 with a color index of 52015. The color of MB is dark green in powder form and deep blue in solution, in which it dissociates into MB cations and chloride anions [14]. The molecular length of MB is 13.82 Å and about 9.5 Å wide [15].

2. Methodology

2.1 Materials

Cellulose acetate (CA) (average Mn = ~30,000 by Gel Permeation Chromatography (GPC); 39.8 wt.% acetyl) was purchased from Sigma-Aldrich (USA). Polyethylene glycol 200 (PEG200) was purchased from Sigma-Aldrich (USA). All the materials were utilized as received, without any further purification.

2.2 CA/PEG200 Beads Preparation

CA was dissolved in dimethyl sulfoxide (DMSO) and acetone in a ratio of 70:30 at 50°C under mechanical stirring for about 1-2 hr. In another beaker, PEG200 was suspended into chloroform and stirred at 50 ^oC for about 30 min. Then, PEG200 solution was added slowly to the CA solution under vigorous stirring and hold at 50 ^oC for about 1 hr. After forming a homogenous solution, the mixture solution was added to distilled water in coagulation bath drop by drop by using a bead maker. The height of apparatus of bead maker and volume of distilled water in coagulation bath were maintained at the same height and volume between all variables to obtain uniform size of beads. The obtained composite CA/PEG200 beads were then immersed in 0.5 N sodium hydroxide (NaOH) solution for 24 h to remove the acetate content. The composite beads were then washed several times using distilled water until obtaining neutral pH condition. Then, the bio-composite beads were dried in an oven at 60–70°C for roughly 4 h. Besides, pure CA beads were prepared with the same procedure, excluding the step of adding PEG200 to the polymer matrix.

2.3 Composite Beads Characterization

The morphology of fracture surface of CA and CA/PEG200 beads were observed using an Inspect S50 Scanning Electron Microscope (SEM). The functional groups of the sample were examined by Fourier Transform-Infrared spectra (FTIR; Spectrum Nicolet iS10 FTIR Spectrometer (Thermo Scientific)). All the infrared spectra were scanned in the range of wavenumber 400-3600 cm^{-1}. X-Ray Diffraction (XRD) analysis was carried out by using a Panalytical X'PERT PRO XRD equipment to inspect the crystal phases of bead samples. The thermal stability of the samples was characterized by Thermogravimetric analyser (TGA; Mettler Toledo).

2.4 Batch Adsorption Evaluation

The adsorption of methylene blue (MB) as cationic dye adsorbate was carried out experimentally in batch system. A series of batch adsorption experiments were executed to observe the effect of operating condition on the MB adsorption onto CA/PEG200 composite beads. Consequently, the adsorption process was examined in various pH (3-11), MB initial concentrations (10-30 mg/L), and adsorbent dosages (1-3 g/L). The PEG200 content in composite beads were also varied to identify its impact on MB adsorption efficacy. Besides, to study kinetic of adsorption, the experiments were carried out at various contact time from 0 to 30 hr, as well as to get the equilibrium adsorption time. Initial and final concentration of MB solution after adsorption at respecting variables were measured by UV-VIS Spectrophotometry (Thermo Genesys10S UV-VIS, USA) at absorbance of 660 nm. Adsorption performance was evaluated from the adsorption capacity (Q, mg/g) and % removal (% R) of MB dye which were calculated by Eq. (1) and (2), respectively, as following

$$Q = \frac{Co - C}{G} \times V \tag{1}$$

$$\%R = \frac{(Co - C) \times 100}{Co} \tag{2}$$

where C_0 is the initial concentration of MB dye (mg/L), C is the final concentration of MB (mg/L), G is the weight of adsorbent beads (g), and V is solution volume (L).

3. Results and Discussion

3.1 SEM Characterization

SEM (Scanning Electron Microscopy) analysis aims to determine the morphology of internal structure of CA and CA/PEG200 (80/20) beads with magnifications of 75 and 15,000, as displayed in Figure 1. The zoom-out images of internal structure of the beads are presented in Figure 1(a) and (b), where it could be seen that the beads show almost spherical shape with some pores and internal interconnected tubular channels. The internal structure of pure CA bead reveals more dense area, while CA/PEG200 (80/20) bead shows more holey structure. For zoom-in SEM images in Figure 1(c), it could be seen that the cross-sectional structure of CA/PEG200 (100/0) beads shows uniform sized and rough porous structure, showing that the surface has more adsorption site for dye (adsorbate). Meanwhile, after the addition of 20 wt.% of PEG200, a typical well-defined porous framework structure with more and bigger pores is observed, as displayed in Figure 1(d). It shows that the addition of PEG200 into CA matrix induced the formation of bigger and more pores in solidified bead obtained from polymer solution, as consequently providing more active site to remove dye. PEG200 is known as plasticizer when it is blended with other polymers (in example: poly(L-lactic acid); PLLA), which can increase the polymer chain mobility [16-18]. Anthanasoulia and Tarantili [16] have reported that the addition of PEG enhances the crystallization ability of PLLA phase due to its lubricating effect which increased mobility of PLLA chains. The more flexible mobility of polymer chain in a solution, the easier movement of solvent from polymer solution to co-solvent in coagulant bath, resulting the more and bigger pores formed inside the beads.

Solid state formation from cellulose solution is accompanied by the replacement between solvent and non-solvent. During solidification process of cellulose beads, the solution on the surface of the cellulose beads is replaced quickly, and the surface of porous bead rapidly forms a film layer, which inhibits the replacement rate of solvent and non-solvent to a certain extent [19].

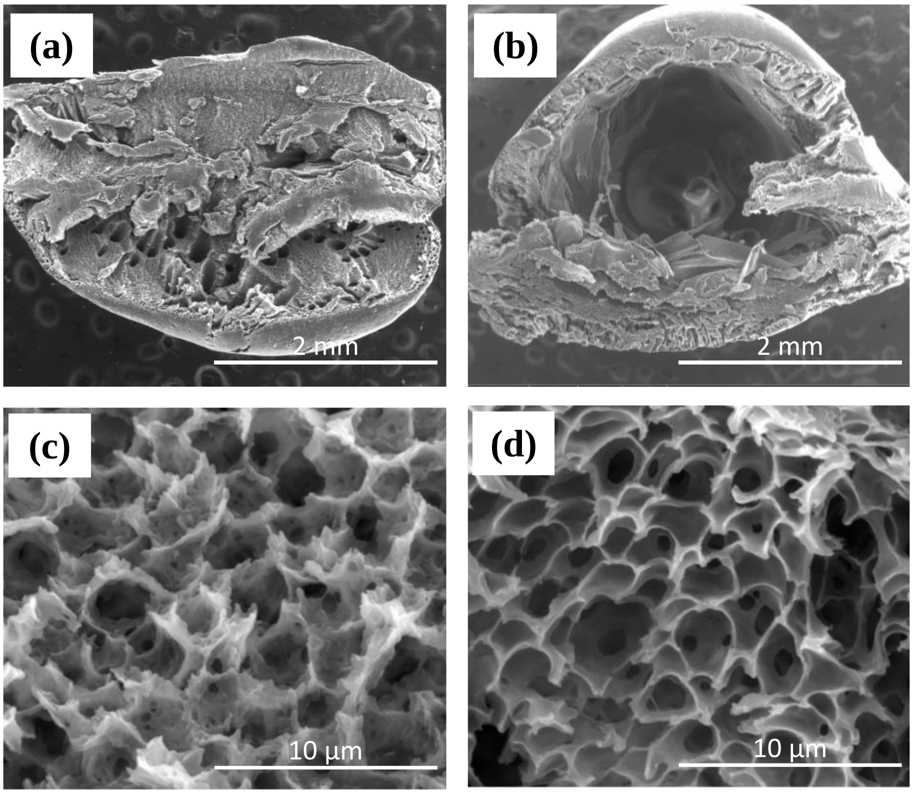

Fig. 1. SEM images of fracture surface of pure CA bead (a, c) and CA/PEG200 (80/20) composite bead (b, d) in magnifications of 75 (top images) and 15,000 (bottom images)

3.2 FTIR Analysis

The FTIR spectra of PEG200, CA, and CA/PEG200 (80/20) are shown in Figure 2. The dominant functional group of PEG200 is hydroxyl group (-OH) located in the wavenumber range of of 3200-3600 cm^{-1}. As shown in Figure 2, -OH group in pristine PEG200 appears at 3391.59 cm^{-1}. Furthermore, the FTIR spectrum of PEG200 points out the absorption peaks at 2866, 1453, 1349, and 1059 cm^{-1}, which correspond to the C_{sp3}-H stretching, C-H bending (1453 and 1349 cm^{-1}), and C-O stretching vibrations, respectively [20].

The CA characteristic peaks are seen at a wavenumber of 3302 corresponding to the hydroxyl functional group, as displayed in Figure 2. Absorption peaks at 2899, 1647, 1416, and 1021 cm^{-1} are also appeared in the spectrum of pure CA beads, which attribute to the C-H stretching in sp^3 hybridization, carbonyl group (C=O), C-H bending, and C-O stretching vibrations, respectively [20].

Molecular structure of CA contains ester functional group indicated the existence of carbonyl groups (C=O) which are usually observed at wavenumber 1735-1750 cm^{-1} [19]. However, in this study, the carbonyl functional groups of CA bead appear at wavenumber of 1647 cm^{-1}. This shift is caused by complete hydrolysis, regenerated, and deacetylation of porous cellulose acetate beads to porous cellulose beads [21]. During dissolution of CA, the intramolecular and intermolecular hydrogen bonding in cellulose structure is broken. And then solidification result in the recombination of new hydrogen bonds in regenerated cellulose [19].

Meanwhile, the FTIR spectrum of CA/PEG200 (80/20) composite beads exhibits almost similar spectrum of pure CA beads. Absorption peaks at 3309, 2899, 1647, 1416, dan 1021 cm^{-1} can be seen in spectrum as demonstrated in Figure 2. Slightly shift of hydroxyl (-OH) group from wavenumber of 3302 to 3309 cm^{-1} is due to small amount interaction of hydrogen bonding between -OH group in PEG200 and C=O group in CA. Unremarkably change in intensity of absorption peaks at 3309, 1647, and 1021 cm^{-1} occurred after 20 wt.% PEG200 addition because of the change in component composition of composite beads. Absorbance peak of C=O and -OH groups become slightly smaller in their intensity, because CA portion is lower in CA/PEG200 (80/20) composite bead than in pure CA bead. It proved that the binary blend forms homogeneous mixture and physical interaction.

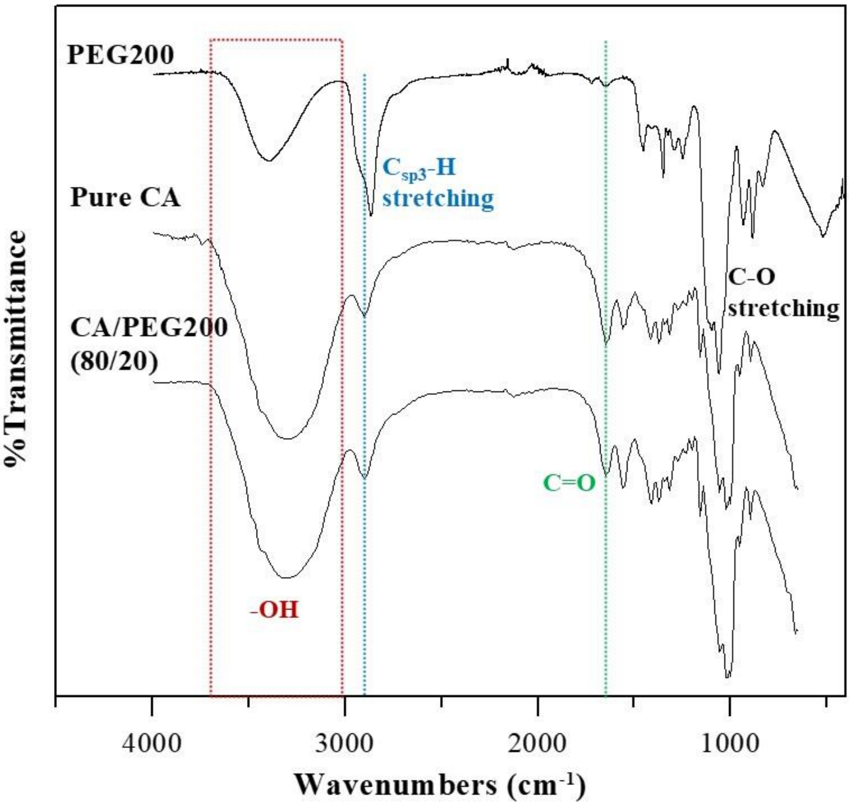

Fig. 2. FTIR spectra of pristine PEG200, pure CA beads, and CA/PEG200 (80/20) composite beads, as indicated *3.3 XRD Analysis*

XRD characterization was carried out for all various bead compositions which aimed to observe the crystallography pattern of cellulose beads, regenerated from CA solution, with the increasing addition of PEG200. Figure 3 depicts the crystalline phase of pure CA and composite CA/PEG200 beads. The XRD pattern of pristine CA beads [CA-PEG200 (100-0)] clarifies its discriminative broad peak at around 2θ = 25° [22], which is assigned to the (002) plane of cellulose II form. Since the CA beads were formed from dissolution and solidification of CA, the hydrogen bond network in CA experienced reconstruction and regeneration, which promotes the formation of cellulose II crystal structure [23]. The broad peak of cellulose crystal phase indicates low crystallinity index or almost amorphous. Meanwhile, the XRD pattern of CA-based hybrid beads also point out the typical broad peak of CA shifted at around 2θ = 21° [22]. Furthermore, the XRD pattern of pure CA and CA/PEG200 beads evinces a structure mostly amorphous, once only broad crystalline peak was observed [24]. The higher content of PEG200, the broader peak of CA/PEG200 beads appear in XRD pattern, showing more amorphous of the crystal phase.

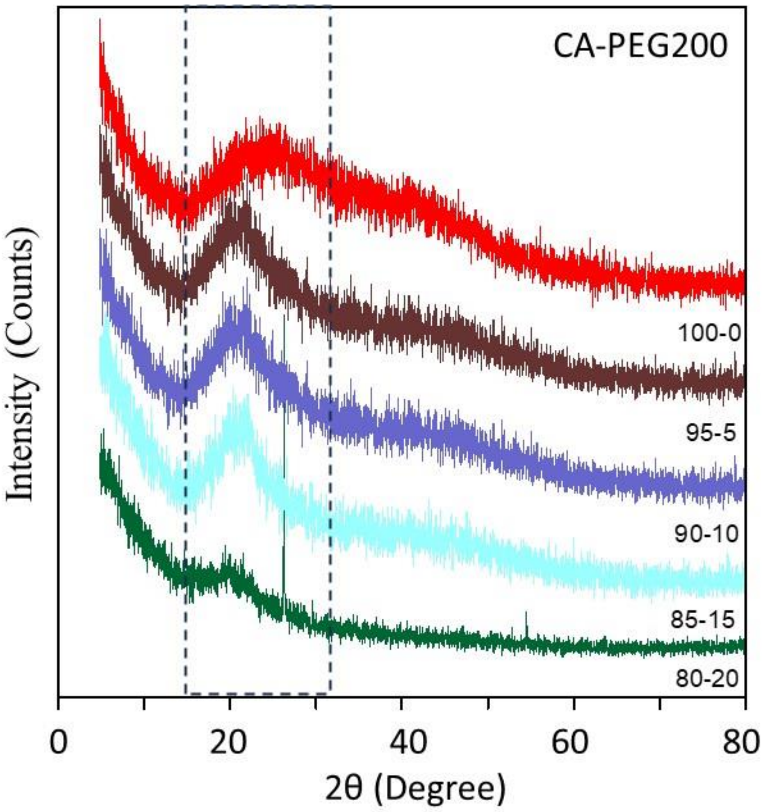

Fig. 3. XRD diffraction patterns of pure CA and composite CA/PEG200 beads with weight ratio as indicated

3.4 Thermal Stability Observation

TGA characterization was carried out to observe thermal stability of regenerated cellulose beads obtained from CA solution and their composites with PEG200, as shown in Figure 4. TGA profiles exhibit three main stages of cellulose degradation and residual degradation. As revealed in TGA curves, pure CA bead displays a significant weight loss at 50-160 °C associated to the bound and internal free water desorption. Second decomposition peak of pure CA bead is observed at between 280-340 °C due to polymer chain degradation. The last step is carbonization and oxidation process which was occurred at 340-800 °C.

Meanwhile, TGA thermogram of CA/PEG200 (80/20) beads in Figure 4 displays a significant different pattern compared to that of pure CA beads. TGA profile shows a slight weight loss at 50-100 °C, elucidated water or moisture vaporization indicating hydrophobic nature of the beads. The significant mass loss between 200-360 °C can be attributed to the polymer chain degradation, which is fragmentation of carbonyl and carboxyl group due to partial pyrolysis [25,26]. The main polymer structure is further decomposed in 360-700 °C region indicating further degradation and carbonization. Then, further carbonization and oxidation of gaseous products occurred at 735 °C to higher temperature. In addition, TGA pattern in Figure 4 shows that the weight residue of CA/PEG200 beads at 800 °C is much higher than that of pure CA beads. This result implies amelioration in thermal stability of composite CA/PEG200 beads compared to pristine CA beads.

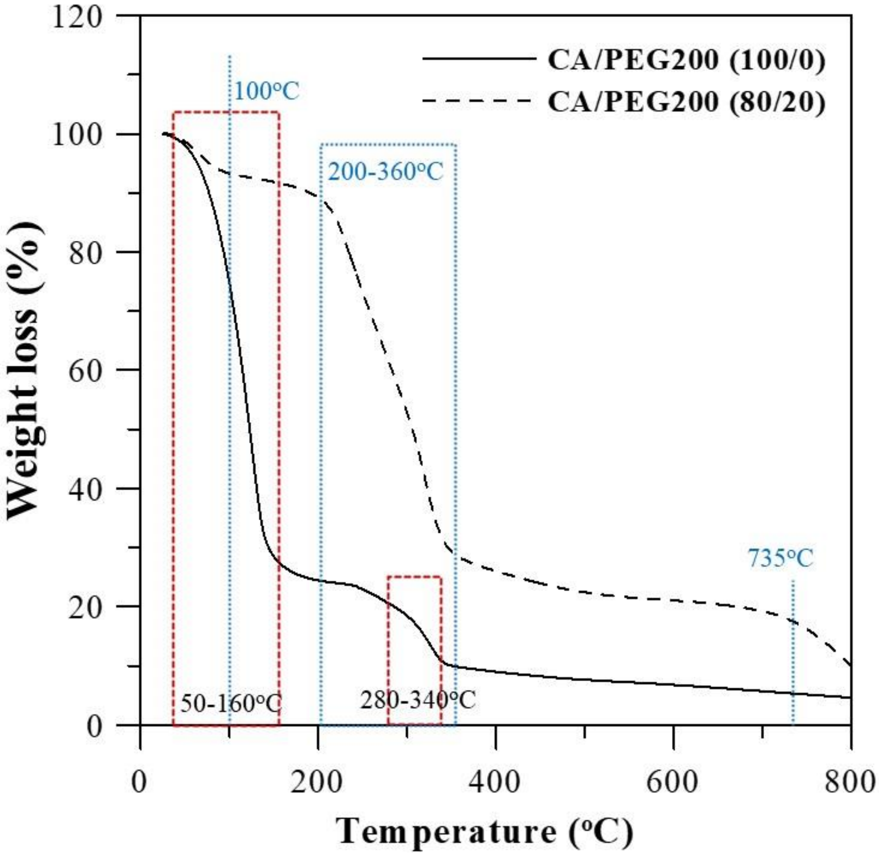

Fig. 4. Thermogravimetry analysis (TGA) curves of pristine CA and CA/PEG200 beads, as indicated

3.5 Batch Adsorption Evaluation

A batch adsorption process was conducted under variation bead compositions and adsorption parameters of time (t), pH, and initial concentration of MB (C_o) to evaluate their effect on adsorption performance. Some operational conditions were kept unchanged for all variables, which are bead dosage of 2 g/L, temperature of 30 °C, and equilibrium time of 24 hr. An experiment under variation of time in batch adsorption was also needed for studying adsorption kinetics of the novel composite beads.

3.5.1 The effect of time on adsorption performance

An adsorption experiment with variation of time was carried out at pH of 7, bead dosage (G) of 2 g/L, initial MB concentration (C_o) of 20 mg/L, and temperature (T) of 30°C, to determine the equilibrium adsorption time for all bead compositions. The concentration of methylene blue (MB) dye was measured every 6 hours until 30 h. In addition, the effect of time was evaluated on adsorption performance in terms of adsorption capacity and % removal as depicted in Figure 5. As we can see in Figure 5, the adsorption capacity (Q) and % removal (%R) of all variable bead compositions increase significantly with the increasing of time until 18 h of adsorption. At longer adsorption time, the Q and %R increase slowly and finally remain constant. The time at which the adsorption capacity remains stable is defined as equilibrium adsorption time. And, the adsorption capacity at equilibrium time is called equilibrium adsorption capacity (Q_e).

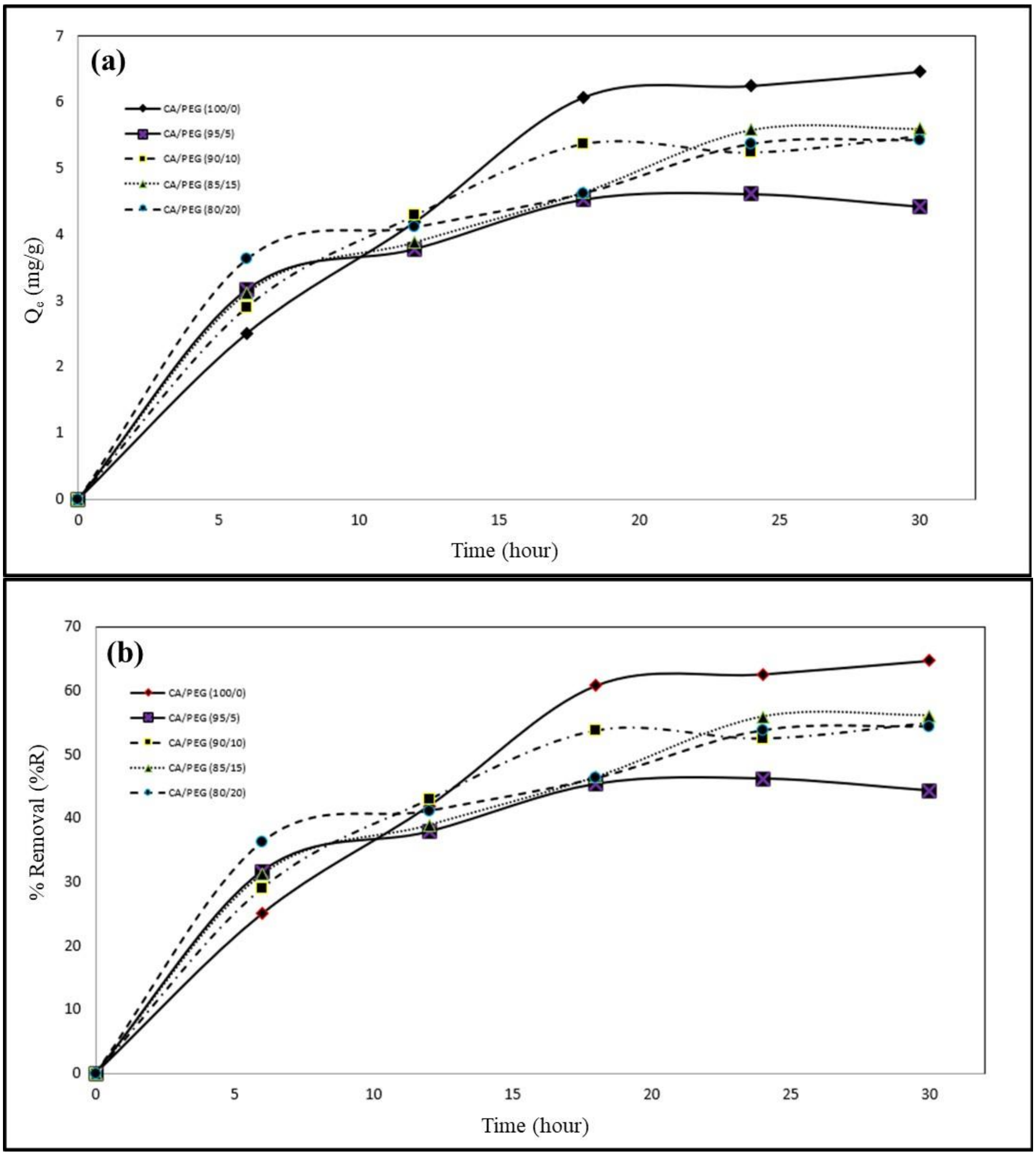

Fig. 5. Effect of time on (a) adsorption capacity and (b) % Removal of Methylene Blue (MB) at C_o=20 mg/L, G=2 g/L, T=30 °C and pH=7 with variation of bead compositions

3.5.2 The effect of beads composition on adsorption process

The equilibrium adsorption process was carried out in 25 ml MB solution at various MB concentration, beads dosage of 2 g/L, temperature 30 °C, pH 7, and for 24 h. Figure 6 displays graphs of adsorption performance (Q and %R) with the variation of PEG200 content and C_o. At lower C_o, the increase in PEG200 content does not result in either Q or %R. However, at higher Co, the Q and %R in general increase with the increasing of PEG200 content. Low concentration of MB contains small amount of solute that can be adsorbed, leading to small value of Q and %R due to more active site available for adsorption. In contrast, high concentration of MB contains large amount of solute which are able to fill the vacant site on the surface of porous beads. Moreover, the increase in MB concentration raises the driving forces of the MB molecules to overcome the mass transfer resistance, leading to the increase in the movement of MB molecules from their solution to bead's surface [27].

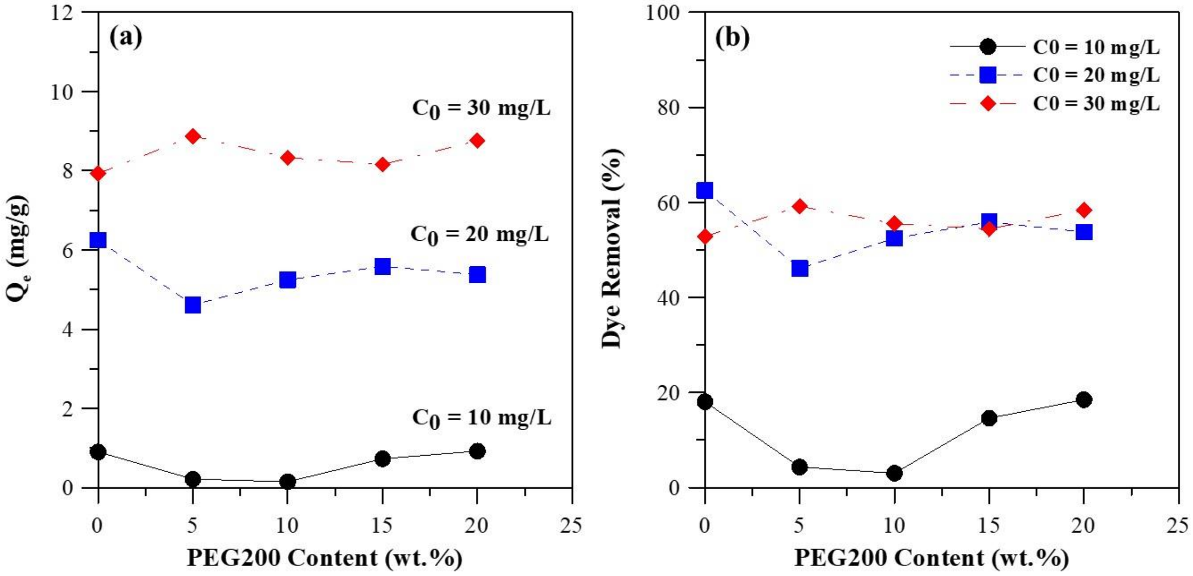

Fig. 6. Effect of PEG200 content on (a) adsorption capacity and (b) % Removal of Methylene Blue (MB) at t=24 h, G=2 g/L, T=30 °C and pH=7 with variation of C_o

3.5.3 The effect of pH of dye solution on adsorption process

The adsorption process was carried out at various pH (3, 7, and 11). The pH of MB solution was adjusted using 1 N HCl and NaOH solutions. Figure 7 shows the graphs revealing the effect of pH on Q and %R of MB on pure CA and composite CA/PEG200 beads. The operational conditions of adsorption were fixed at C_o of 20 mg/L, bead dosage of 2 g/L, and temperature of 30°C for 24 h. As seen in Figure 7, the increase in pH also improves Q and %R of MB on all variable bead compositions. Indeed, pH of solution plays important role in adsorption since it influences the charge of adsorbent surface. At high pH (basic solution), the surface of cellulose-based beads become more negatively charged. Consequently, the stronger electrostatic interaction between negatively charged cellulose beads and cationic MB. This result was in line with the earlier research by Eltaweil *et al.,* [26] that also evinced the enhancement of Q and %R of MB with the raising of pH medium.

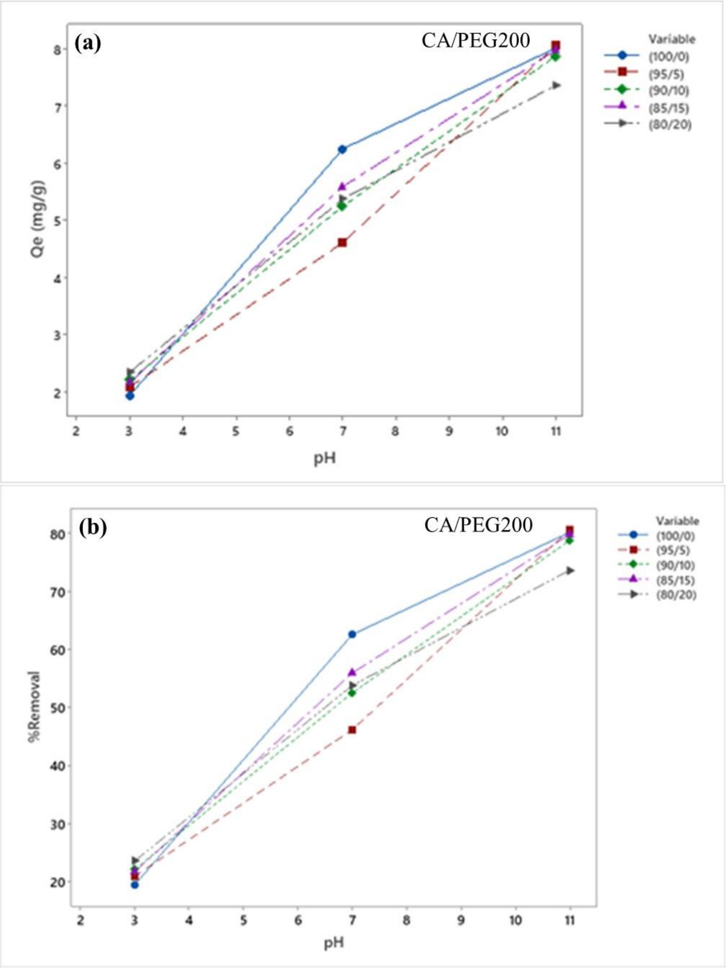

Fig. 7. Effect of pH on (a) adsorption capacity and (b) % Removal of Methylene Blue (MB) at C_o=20 mg/L, G=2 g/L, T=30 °C, and t=30 h with variation of bead compositions

3.5.4 The effect of initial concentration of dye solution on adsorption performance

An experiment of batch adsorption at various initial concentrations of MB (C_o) was conducted for all variables of bead composition to examine their effect on Q and %R of MB on cellulose-based adsorbent beads. Initial MB or solute concentration is one of the key parameters to investigate the efficacy of adsorbent materials. Figure 8 demonstrates the impact of initial concentration of MB dye on adsorption performance of beads. It is presented in Figure 8 that the raise in C_o results in the increase in Q and %R. This trend appears on the adsorption performance of almost all CA/PEG200 beads. However, the dye removal percentage is declined as per increase in C_o above 20 mg/L for pure CA and CA/PEG200 (85/15) beads. The decrease in %R might be caused of MB desorption. At high dye concentration, the adsorption occurs rapidly so that the adsorbent cannot adsorb further, as the active sites have been already full. Finally, in longer adsorption time, the fully adsorbed adsorbents could release back the solute to the dye solution called desorption. Therefore, it is important to evaluate the equilibrium adsorption time of a specific adsorbent.

After comparing the adsorption performance of adsorbent beads for MB removal in batch system for all variables (bead compositions and operational conditions), the best performance was demonstrated by the biocomposite CA/PEG200 (80/20) bead at pH of 11, dosage bead of 1 g/L, and initial MB concentration of 30 mg/L. The best % removal and adsorption capacity of MB were 93.35 % and 28.005 mg/g, respectively.

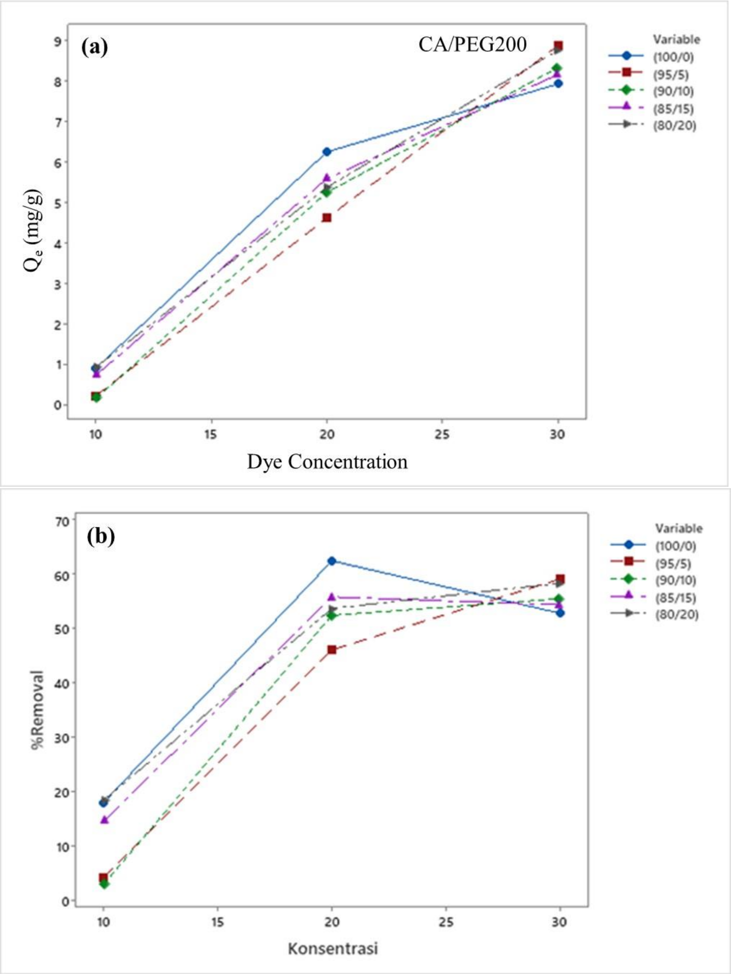

Fig. 8. Effect of initial concentration of MB (C_o) on (a) adsorption capacity and (b) % Removal of Methylene Blue (MB) at pH=7, G=2 g/L, T=30 °C, and t=30 h with variation of bead compositions

3.6 Kinetic Study of The Adsorption

Adsorption kinetics investigates the interaction between adsorbate and adsorbent interaction and depends on the adsorption condition. Different kinetic models were utilized to determine the adsorption rate–determining steps and the mechanism of the adsorbate on adsorbent [28-32]. Moreover, modelling of adsorption kinetics is of paramount importance to describe the experimental data and to predict the results for conditions beyond those treated experimentally [33]. Lagergren's kinetics equation was the most commonly used for the batch adsorption process. In this study, the experimental data was analysed and fitted to three different kinetic models: the so-called pseudo-first order model (PFO), the pseudo-second order model (PSO), and the Elovich model. The kinetic data were collected in every 6 h at batch adsorption conditions of C_o=20 mg/L, G=2 g/L, T= 30 °C, and pH= 7.

The kinetic model of Pseudo first order (PSO) is described by the Lagergren kinetic equation, as shown in Eq. (3)

$$\log(q_e - q_t) = \log q_e - \left(\frac{k_1}{2{,}303}\right) t \tag{3}$$

where, q_t is the adsorption capacity at time t (mg/g), k_1 defines rate constant for first order kinetics (h^{-1}), and t is contact time (hour), q_e represents equilibrium adsorption capacity (mg/g) which was obtained from solver after trial q_e for linear relationship of $\log(q_e\text{-}q_t)$ vs. t. Then, k_1 could be obtained from the slope of linear equation. The Pseudo-second order (PSO) kinetic is expressed as written in Eq. (4)

$$\frac{t}{qt} = \left(\frac{1}{k2.qe^2}\right) + \left(\frac{1}{qe}\right) t \tag{4}$$

where, k_2 symbolizes rate constant of second order kinetic (g/mg). The amount of dye adsorbed at equilibrium time (q_e) and k_2 were obtained from the linear relationship of t/qt vs. t. Meanwhile, the Elovich kinetic model is also often used to describe adsorption kinetics. The Elovich equation model is written as seen in Eq. (5) [34]

$$qt = \left(\frac{1}{\beta}\right) \ln(\alpha.\beta) + \left(\frac{1}{\beta}\right) \ln t \tag{5}$$

where, q_t is the amount of dye adsorbed by adsorbent at time t (mg/g). The others (α and β) represent the parameters of the Elovich model during any an experiment. The parameters α and β are defined as initial rate of adsorption and desorption constant, respectively [35].

To evaluate which kinetic models fitted well to experimental data, correlation coefficient (R^2) was determined from calculation or linear graph of each model. Higher value of R^2 (closer to unity) showed the more fitted experimental data to the model. Data of constant values, parameters, and R^2 of each kinetic model for all variable bead composition were tabulated in Tabel 1. Figure 9-11 show the plot of experimental data fitted to Pseodu-first order (PFO), Pseodu-second order (PSO), and Elovich kinetic models, respectively. In average, the smallest value of R^2 is for Pseodu-first order (PFO) kinetic model showing impropriety of this model to experimental data. On the other hand, Elovich kinetic model demonstrates highest value of R^2, as listed in Table 1. This implies that the experiment data of MB adsorption on CA/PEG200 beads adsorbent can be well described by using Elovich equation model, reflecting the nature of chemical adsorption. In engineering practice, it is important to determine an efficient adsorption time for the batch adsorption system suitably described by the Elovich kinetic model. In general speaking, the result in this study provides a potential of using biosorbent in waste water treatment which follow the principles of sustainable development by utilizing biodegradable and renewable materials [36].

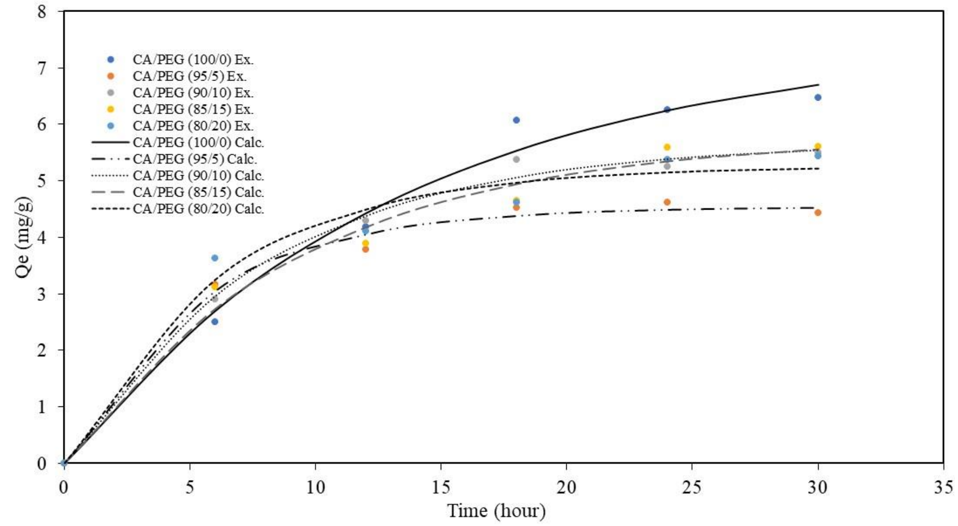

Fig. 9. Plot of adsorption data fitted to Pseudo-First Order Kinetics Model

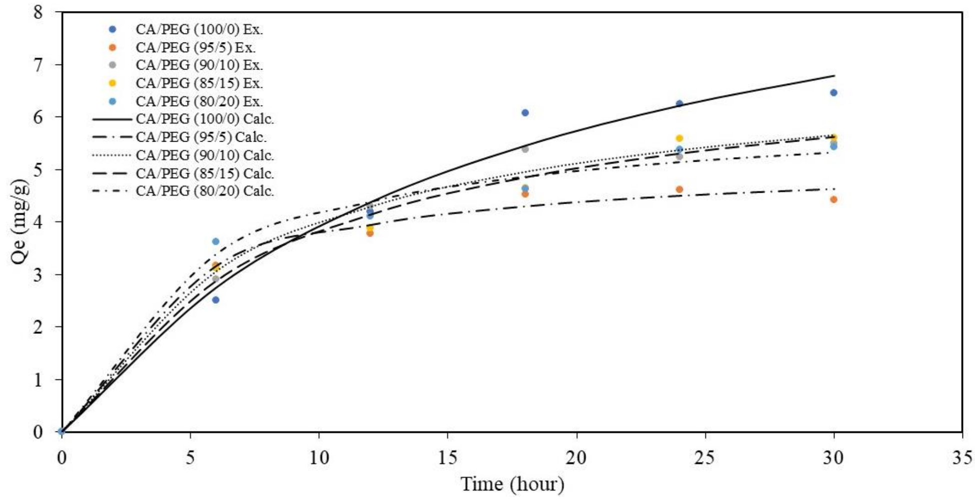

Fig. 10. Plot of adsorption data fitted to Pseudo-Second Order Kinetics Model

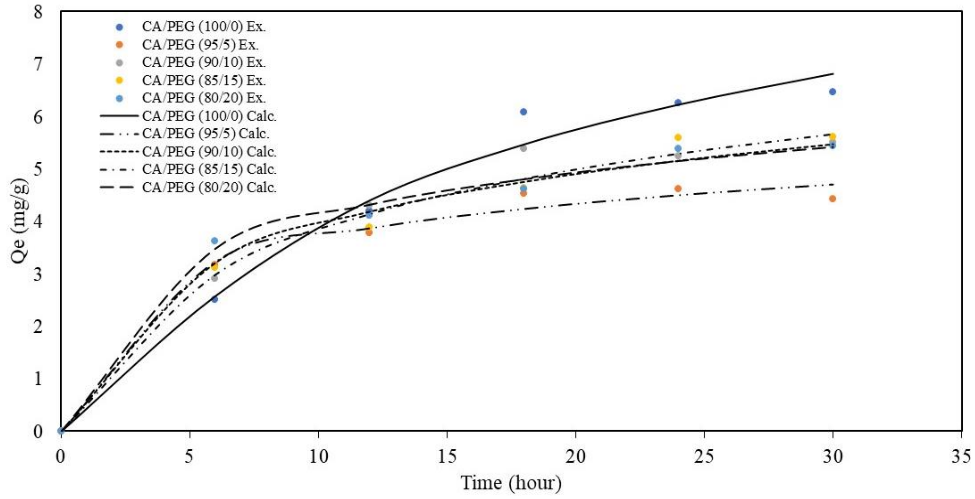

Fig. 11. Plot of adsorption data fitted to Elovich Kinetics Model

Table 1
Parameters of MB Dyes Adsorption Kinetics by CA/PEG Beads

Parameter kinetics	CA/PEG200 (100/0)	CA/PEG200 (95/5)	CA/PEG200 (90/10)	CA/PEG200 (85/15)	CA/PEG200 (80/20)	AVG
Pseudo-first order						
Qe (mg. g^{-1})	7.504	4.543	5.689	5.791	5.264	
k1 (h^{-1})	0.074	0.185	0.123	0.107	0.160	
R^2	0.910	0.685	0.805	0.840	0.729	0.794
Pseudo-second order						
Qe (mg. g^{-1})	10.706	5.230	7.176	7.377	6.222	
k2 (h^{-1})	0.005	0.049	0.017	0.015	0.0322	
R^2	0.918	0.700	0.820	0.842	0.7406	0.804
Elovich Equation						
α (mmol/g.min)	1.169	5.302	2.318	1.671	3.651	
β (g/mmol)	0.381	1.10	0.713	0.603	0.834	
R^2	0.923	0.913	0.795	0.839	0.749	0.844

4. Conclusions

Biocomposite beads were successfully prepared from the mixture of cellulose acetate and polyethylene glycol 200 (CA/PEG200) for adsorption of methylene blue (MB) in batch systems. The adsorption performance of biocomposite beads was improved with the increasing content of PEG200. The basic conditions are favourable for adsorption of MB by CA/PEG200 beads. The negatively charged of cellulose-based bead’s surface in high pH (basic condition) provided more electrostatic interaction between cellulose beads and cationic MB. Adsorption performance was also enhanced when occurred in high initial MB concentration of 30 mg/L because it contains large amount of solute which are able to fill the vacant site on the surface of porous beads. The best adsorption performance was reached at condition of pH 11, initial MB concentration 30 mg/L, and bead dosage 1 g/L for biocomposite CA/PEG200 (80/20) bead, with % MB removal and adsorption capacity of 93.35 % and 28.005 mg/g, respectively. The appropriate kinetic model to describe the adsorption of MB on CA/PEG200 beads was Elovich kinetic model, demonstrating the presence of chemisorption in the adsorption process.

Acknowledgement

The authors would like to express their gratitude to the Indonesian Ministry of Research, Technology, and Higher Education (DIKTI) (Grant contract No. 2097/PKS/ITS/2022), which financially supported this research for one consecutive year.

References

[1] Hokkanen, Sanna, Amit Bhatnagar, and Mika Sillanpaa. “A review on modification methods to cellulose-based adsorbents to improve adsorption capacity.” *Water Research* 91, (2016): 156-173. https://doi.org/10.1016/j.watres.2016.01.008

[2] Ahmad, A. A., B. H. Hameed, and N. Aziz. "Adsorption of direct dye on palm ash: Kinetic and equilibrium modeling." *Journal of hazardous materials* 141, no. 1 (2007): 70-76. https://doi.org/10.1016/j.jhazmat.2006.06.094

[3] Kumar, K. Vasanth. "Linear and non-linear regression analysis for the sorption kinetics of methylene blue onto activated carbon." *Journal of hazardous materials* 137, no. 3 (2006): 1538-1544. https://doi.org/10.1016/j.jhazmat.2006.04.036

[4] Rafatullah, Mohd, Othman Sulaiman, Rokiah Hashim, and Anees Ahmad. "Adsorption of methylene blue on low-cost adsorbents: a review." *Journal of hazardous materials* 177, no. 1-3 (2010): 70-80. https://doi.org/10.1016/j.jhazmat.2009.12.047

[5] Idris, Ani, and Lee Kuan Yet. "The effect of different molecular weight PEG additives on cellulose acetate asymmetric dialysis membrane performance." *Journal of Membrane Science* 280, no. 1-2 (2006): 920-927. https://doi.org/10.1016/j.memsci.2006.03.010

[6] Gericke, Martin, Jani Trygg, and Pedro Fardim. "Functional cellulose beads: preparation, characterization, and applications." *Chemical reviews* 113, no. 7 (2013): 4812-4836. https://doi.org/10.1021/cr300242j

[7] Ni'mah, Hikmatun, Desy Puspitasari, Akhmad Reski Kurniawan, Burhanudin Muiz, Achmad Roesyadi, Firman Kurniawansyah, and Eva Oktavia Ningrum. "Kinetic study of cationic dye adsorption on cellulose acetate butyrate/poly (L-lactic acid) composite beads." In *AIP Conference Proceedings*, vol. 2197, no. 1. AIP Publishing, 2020. https://doi.org/10.1063/1.5140959

[8] Rofaudin, Muhammad Naufal Fatkhi, Azizul Pradna Qoidani, Desy Puspitasari, Helmi Kurnia Arnanda, Hikmatun Ni'mah, Achmad Roesyadi, Firman Kurniawansyah, and Eva Oktavia Ningrum. "Prediction of continuous adsorption performance of cellulose acetate butyrate/poly (L-lactid acid) composite beads for dye removal." In *IOP Conference Series: Materials Science and Engineering*, vol. 1053, no. 1, p. 012008. IOP Publishing, 2021. https://doi.org/10.1088/1757-899X/1053/1/012008

[9] Caesario, Bonifacius Andhra Dwima, Muhammad Dava Rachmadi Ali, Desy Puspitasari, Helmi Kurnia Arnanda, Hikmatun Ni'mah, Firman Kurniawansyah, and Eva Oktavia Ningrum. "Cellulose-Based beads for cationic dye removal in continuous adsorption." *Materials Today: Proceedings* 63 (2022): S354-S358. https://doi.org/10.1016/j.matpr.2022.03.547

[10] Ni'mah, Hikmatun, and Eamor M. Woo. "Coexisting Straight, Radial, and Banded Lamellae on the Six Corners of Hexagon-Shaped Spherulites in Poly (l-Lactide)." *Macromolecular Chemistry and Physics* 215, no. 19 (2014): 1838-1847. https://doi.org/10.1002/macp.201400211

[11] Ni'mah, Hikmatun, Rochmadi Rochmadi, Eamor M. Woo, Dian A. Widiasih, and Siska Mayangsari. "Preparation and Characterization of Poly (L-Lactic Acid) Films Plasticized with Glycerol and Maleic Anhydride." *International Journal of Technology* 10, no. 3 (2019): 531-540. https://doi.org/10.14716/ijtech.v10i3.2936

[12] Fischer, Steffen, Katrin Thümmler, Bert Volkert, Kay Hettrich, Ingeborg Schmidt, and Klaus Fischer. "Properties and applications of cellulose acetate." In *Macromolecular symposia*, vol. 262, no. 1, pp. 89-96. Weinheim: WILEY-VCH Verlag, 2008. https://doi.org/10.1002/masy.200850210

[13] Loprieno, N. "International Agency for Research on Cancer (IARC) monographs on the evaluation of carcinogenic risk of chemicals to man:" relevance of data on mutagenicity"." *Mutation research* 31, no. 3 (1975): 210. https://doi.org/10.1016/0165-1161(75)90092-8

[14] Raposo Bejines, Francisco, M. Rubia, and Rafael Borja Padilla. "Methylene blue number as useful indicator to evaluate the adsorptive capacity of granular activated carbon in batch mode: Influence of adsorbate/adsorbent mass ratio and particle size." (2009). https://doi.org/10.1016/j.jhazmat.2008.09.106

[15] Jia, Puqi, Hongwei Tan, Kuiren Liu, and Wei Gao. "Removal of methylene blue from aqueous solution by bone char." *Applied sciences* 8, no. 10 (2018): 1903. https://doi.org/10.3390/app8101903

[16] Athanasoulia, Ioanna-Georgia, and Petroula A. Tarantili. "Preparation and characterization of polyethylene glycol/poly (L-lactic acid) blends." *Pure and Applied Chemistry* 89, no. 1 (2017): 141-152. https://doi.org/10.1515/pac-2016-0919

[17] Sungsanit, K. U. L. L. A. W. A. D. E. E., Nhol Kao, and S. N. Bhattacharya. "Properties of linear poly (lactic acid)/polyethylene glycol blends." *Polymer engineering & science* 52, no. 1 (2012): 108-116. https://doi.org/10.1002/pen.22052

[18] Baiardo, Massimo, Giovanna Frisoni, Mariastella Scandola, Michel Rimelen, David Lips, Kurt Ruffieux, and Erich Wintermantel. "Thermal and mechanical properties of plasticized poly (L-lactic acid)." *Journal of Applied Polymer Science* 90, no. 7 (2003): 1731-1738. https://doi.org/10.1002/app.12549

[19] Xia, Yuanyuan, Xinping Li, Yue Yuan, Jingshun Zhuang, and Wenliang Wang. "A Facile Way for Preparation of Cellulose Beads With High Homogeneity, Low Crystallinity, and Tunable-Internal Structure." (2021). https://doi.org/10.21203/rs.3.rs-673294/v1

[20] Wade, Leroy G., Jr. *Organic chemistry* 6th Ed. New Jersey: Pearson education, Inc., 2006.

[21] Bai, Yong-Xiao, and Yan-Feng Li. "Preparation and characterization of crosslinked porous cellulose beads." *Carbohydrate polymers* 64, no. 3 (2006): 402-407. https://doi.org/10.1016/j.carbpol.2005.12.009

[22] Mohiuddin, Md, Kishor Kumar Sadasivuni, Seongcheol Mun, and Jaehwan Kim. "Flexible cellulose acetate/graphene blueprints for vibrotactile actuator." *RSC Advances* 5, no. 43 (2015): 34432-34438. https://doi.org/10.1039/C5RA03043A

[23] Mystek, Katarzyna, Michael S. Reid, Per A. Larsson, and Lars Wågberg. "In situ modification of regenerated cellulose beads: creating all-cellulose composites." *Industrial & Engineering Chemistry Research* 59, no. 7 (2020): 2968-2976. https://doi.org/10.1021/acs.iecr.9b06273

[24] Kamal, M., E. M. Abdelrazek, N. M. Sellow, and A. M. Abdelghany. "Synthesis and optimization of novel chitosan/cellulose acetate natural polymer membrane for water treatment." *Journal of Advances in Physics* 14, no. 1 (2018): 5303-5311. https://doi.org/10.24297/jap.v14i1.7183

[25] Barud, Hernane S., Adalberto M. de Araújo Júnior, Daniele B. Santos, Rosana MN de Assunção, Carla S. Meireles, Daniel A. Cerqueira, Guimes Rodrigues Filho, Clóvis A. Ribeiro, Younes Messaddeq, and Sidney JL Ribeiro. "Thermal behavior of cellulose acetate produced from homogeneous acetylation of bacterial cellulose." *Thermochimica acta* 471, no. 1-2 (2008): 61-69. https://doi.org/10.1016/j.tca.2008.02.009

[26] Eltaweil, Abdelazeem S., Eman M. Abd El-Monaem, Gehan M. El-Subruiti, Bassma M. Ali, Mona M. Abd El-Latif, and Ahmed M. Omer. "Graphene oxide incorporated cellulose acetate beads for efficient removal of methylene blue dye; isotherms, kinetic, mechanism and co-existing ions studies." *Journal of Porous Materials* 30, no. 2 (2023): 607-618. https://doi.org/10.1007/s10934-022-01347-6

[27] Omer, Ahmed M., Eman M. Abd El-Monaem, Gehan M. El-Subruiti, Mona M. Abd El-Latif, and Abdelazeem S. Eltaweil. "Fabrication of easy separable and reusable MIL-125 (Ti)/MIL-53 (Fe) binary MOF/CNT/Alginate composite microbeads for tetracycline removal from water bodies." *Scientific reports* 11, no. 1 (2021): 23818. https://doi.org/10.1038/s41598-021-03428-z

[28] Lagergren, S. Kung. "About the theory of so-called adsorption of soluble substances." *Sven. Vetenskapsakad. Handingarl* 24 (1898): 1-39.

[29] Blanchard, G., M. Maunaye, and G. Martin. "Removal of heavy metals from waters by means of natural zeolites." *Water research* 18, no. 12 (1984): 1501-1507. https://doi.org/10.1016/0043-1354(84)90124-6

[30] Aharoni, C., and F. C. Tompkins. "Kinetics of adsorption and desorption and the Elovich equation." In *Advances in catalysis*, vol. 21, pp. 1-49. Academic Press, 1970. https://doi.org/10.1016/S0360-0564(08)60563-5

[31] Helfferich, F. "Equilibria; Kinetics; Ion-Exchange in Columns." *Ion Exchange; Series in Advanced Chemistry; McGraw-Hill Book Company: New York, NY, USA* (1962): 95-322.

[32] Weber Jr, Walter J., and J. Carrell Morris. "Kinetics of adsorption on carbon from solution." *Journal of the sanitary engineering division* 89, no. 2 (1963): 31-59. https://doi.org/10.1061/JSEDAI.0000430

[33] Kyzas, George Z., Margaritis Kostoglou, and Nikolaos K. Lazaridis. "Copper and chromium (VI) removal by chitosan derivatives—Equilibrium and kinetic studies." *Chemical Engineering Journal* 152, no. 2-3 (2009): 440-448. https://doi.org/10.1016/j.cej.2009.05.005

[34] Wu, Feng-Chin, Ru-Ling Tseng, and Ruey-Shin Juang. "Characteristics of Elovich equation used for the analysis of adsorption kinetics in dye-chitosan systems." *Chemical Engineering Journal* 150, no. 2-3 (2009): 366-373. https://doi.org/10.1016/j.cej.2009.01.014

[35] Cea, M., J. C. Seaman, A. Jara, M. L. Mora, and M. C. Diez. "Kinetic and thermodynamic study of chlorophenol sorption in an allophanic soil." *Chemosphere* 78, no. 2 (2010): 86-91. https://doi.org/10.1016/j.chemosphere.2009.10.040

[36] Nandiyanto, Asep Bayu Dani, Meli Fiandini, Denaya Ayu Fadiah, Pitri Aprilia Muktakin, Risti Ragadhita, Willy Cahya Nugraha, Teguh Kurniawan, Muhammad Roil Bilad, Jumril Yunas, and Abdulkareem Sh Mahdi Al Obaidi. "Sustainable Biochar Carbon Microparticles Based on Mangosteen Peel as Biosorbent for Dye Removal: Theoretical Review, Modelling, and Adsorption Isotherm Characteristics." *Journal of Advanced Research in Fluid Mechanics and Thermal Sciences* 105, no. 1 (2023): 41-58. https://doi.org/10.37934/arfmts.105.1.4158